Neurobiology of Disease 171 (2022) 105803

Contents lists available at ScienceDirect

Neurobiology of Disease

journal homepage: www.elsevier.com/locate/ynbdi

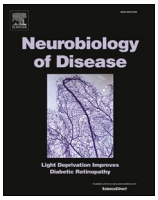

Mitochondrial electron transport chain defects modify Parkinson's disease phenotypes in a *Drosophila* model

Maria E. O'Hanlon [a,b], Clare Tweedy [c,1], Filippo Scialo [d,2,3], Rosemary Bass [e], Alberto Sanz [d,4], Tora K. Smulders-Srinivasan [a,b,e,*]

[a] School of Health & Life Sciences, Teesside University, Middlesbrough TS1 3BX, United Kingdom
[b] National Horizons Centre, Teesside University, Darlington DL1 1HG, United Kingdom
[c] Biosciences Institute, Newcastle University, Medical School, Framlington Place, Newcastle-upon-Tyne NE2 4HH, UK
[d] Institute for Cell and Molecular Biosciences, Newcastle University Institute for Ageing, Newcastle University, Campus for Ageing and Vitality, Newcastle upon Tyne NE4 5PL, United Kingdom
[e] Department of Applied Sciences, Faculty of Health and Life Sciences, Northumbria University, Newcastle upon Tyne NE1 8ST, UK

ARTICLE INFO

Keywords:
Mitochondria
electron transport chain
Oxidative phosphorylation
Parkin
PINK1
Cyclope
COX5A
Parkinson's disease
Drosophila melanogaster
Fruit flies

ABSTRACT

Introduction: Mitochondrial defects have been implicated in Parkinson's disease (PD) since complex I poisons were found to cause accelerated parkinsonism in young people in the early 1980s. More evidence of mitochondrial involvement arose when many of the genes whose mutations caused inherited PD were discovered to be subcellularly localized to mitochondria or have mitochondrial functions. However, the details of how mitochondrial dysfunction might impact or cause PD remain unclear. The aim of our study was to better understand mitochondrial dysfunction in PD by evaluating mitochondrial respiratory complex mutations in a *Drosophila melanogaster* (fruit fly) model of PD.

Methods: We have conducted a targeted heterozygous enhancer/suppressor screen using *Drosophila* mutations within mitochondrial electron transport chain (ETC) genes against a null PD mutation in *parkin*. The interactions were assessed by climbing assays at 2–5 days as an indicator of motor function. A strong enhancer mutation in *COX5A* was examined further for L-dopa rescue, oxygen consumption, mitochondrial content, and reactive oxygen species. A later timepoint of 16–20 days was also investigated for both *COX5A* and a suppressor mutation in *cyclope*. Generalized Linear Models and similar statistical tests were used to verify significance of the findings.

Results: We have discovered that mutations in individual genes for subunits within the mitochondrial respiratory complexes have interactions with *parkin*, while others do not, irrespective of complex. One intriguing mutation in a complex IV subunit (*cyclope*) shows a suppressor rescue effect at early time points, improving the gross motor defects caused by the PD mutation, providing a strong candidate for drug discovery. Most mutations, however, show varying degrees of enhancement or slight suppression of the PD phenotypes. Thus, individual mitochondrial mutations within different oxidative phosphorylation complexes have different interactions with PD with regard to degree and direction. Upon further investigation of the strongest enhancer (*COX5A*), the mechanism by which these interactions occur initially does not appear to be based on defects in ATP production, but rather may be related to increased levels of reactive oxygen species.

Abbreviations: AR-JP, autosomal recessive juvenile Parkinsonism; ATP5F1A, mitochondrial complex V ATP synthase; *blw*, *bellwether*; CI, mitochondrial respiratory complex I; CII, mitochondrial respiratory complex II; CIII, mitochondrial respiratory complex III; CIV, mitochondrial respiratory complex IV; *cype*, *cyclope*; *Cyt-c1*, *cytochrome c1*; ETC, electron transport chain; GWAS, genome-wide association studies; H_2DCF, 2′,7’-Dichlorofluorescein; ILBD, incidental Lewy body disease; MPTP, 1-methyl-4-phenyl-1,2,3,6-tetrahydropyridine; *park*, *parkin*; PBS, phosphate-buffered saline; PD, Parkinson's disease; PINK1, PTEN-induced putative kinase 1; ROS, reactive oxygen species; UQCR-C2, *ubiquinol-cytochrome c reductase core protein 2*.

* Corresponding author at: School of Health & Life Sciences, Teesside University, Middlesbrough TS1 3BX, United Kingdom.
E-mail addresses: M.O'Hanlon@tees.ac.uk (M.E. O'Hanlon), c.tweedy@leeds.ac.uk (C. Tweedy), filippo.scialo@unicampania.it (F. Scialo), r.bass@uea.ac.uk (R. Bass), alberto.sanzmontero@glasgow.ac.uk (A. Sanz), t.smulders@tees.ac.uk (T.K. Smulders-Srinivasan).
[1] Present address: School of Biomedical Sciences, Faculty of Biological Sciences, University of Leeds, Leeds, LS2 9JT, United Kingdom.
[2] Present address: Dipartimento di Scienze Mediche Traslazionali, University of Campania “L. Vanvitelli”, Naples, Italy.
[3] Present address: CEINGE, Biotecnologie Avanzate, Naples, Italy.
[4] Present address: Institute of Molecular, Cell and Systems Biology, College of Medical, Veterinary and Life Sciences, University of Glasgow, G12 8QQ, Glasgow, United Kingdom.

https://doi.org/10.1016/j.nbd.2022.105803
Received 10 March 2022; Received in revised form 21 June 2022; Accepted 22 June 2022
Available online 25 June 2022

Conclusions: Our work highlights some key subunits potentially involved in mechanisms underlying PD pathogenesis, implicating ETC complexes other than complex I in PD.

1. Introduction

Mitochondria have been implicated in Parkinson's disease for many years (reviewed in Borsche et al., 2021), with the first evidence arising from unintentional exposure to mitochondrial complex I poisons. Illicit drug consumption led to chronic Parkinsonism in young people, which included the characteristic loss of dopaminergic neurons due to by-products (1-methyl-4-phenyl-1,2,3,6-tetrahydropyridine; MPTP), subsequently discovered to cause complex I inhibition (Davis et al., 1979; Langston et al., 1983; Langston et al., 1999; Ramsay et al., 1986). In addition, high frequencies of atypical Parkinsonism may be caused by the intake of herbal teas and fruits from plants of the Annonaceae family in Guadeloupe containing annonacin, which also blocks complex I (Caparros-Lefebvre and Elbaz, 1999; Champy et al., 2004; Lannuzel et al., 2003; Schapira, 2010).

Genes that have been identified as pathologically mutated within families with hereditary PD (only 5–15% of cases) add to the evidence, as many of them code for proteins with mitochondrial localization and function (Borsche et al., 2021; Bose and Beal, 2016). Alpha-synuclein (SNCA) was the first gene identified in familial PD and the encoded protein is a major constituent of Lewy bodies (Polymeropoulos et al., 1997; Spillantini et al., 1997). Alpha-synuclein null mice were found to be resistant to neurotoxicity when exposed to mitochondrial complex I inhibitor MPTP and over-expression of human alpha-synuclein in mice causes increased sensitivity to MPTP (Dauer et al., 2002; Klivenyi et al., 2006; Nieto et al., 2006; Song et al., 2004). Pathogenic alpha-synuclein can also bind to mitochondria and disrupt cellular respiration (reviewed in Rocha et al., 2018; Wang et al., 2019).

Similarly, Parkin (PRKN) is an E3 ubiquitin ligase for which over 100 pathological mutations have been found and these mutations cause the majority of autosomal recessive PD, usually earlier onset autosomal recessive juvenile Parkinsonism (AR-JP) (Exner et al., 2012; Kitada et al., 1998; Shimura et al., 2000). PINK1 (PTEN-induced putative kinase 1), a serine/threonine-protein kinase, was also identified as mutated in autosomal recessive PD, and may recruit Parkin to defective mitochondria to target them for mitophagy (mitochondrial autophagy) (reviewed in Imai, 2020; Valente et al., 2004). Ceramide accumulation in mitochondria may also be involved with PINK1 pathogenesis (Vos et al., 2021). More PD genes, including DJ-1, LRRK2, and HTRA2, have also been found with varying degrees of relevance to mitochondrial dysfunction in PD (reviewed in Borsche et al., 2021; Keane et al., 2011). Thus, substantial evidence exists that mitochondria play a role in PD, but the mechanism by which they are involved is unclear.

The causes of the more common sporadic PD are complex, with environmental and genetic susceptibilities both involved, though the biggest risk factor is ageing (Rodríguez-Nogales et al., 2016; Van Den Eeden et al., 2003). Genome-wide association studies (GWAS) and other association studies have also implicated mitochondrial genes/pathways as being risk factors for PD (Billingsley et al., 2019; Dumitriu et al., 2016; Hall et al., 2020). Suggestively, mitochondrial dysfunction is also associated with sporadic cases of PD. Patients show a decrease in activity of mitochondrial complex I in the substantia nigra and the frontal cortex brain regions as well as other tissues (Bindoff et al., 1991; Haas et al., 1995; Parker Jr et al., 2008; Schapira et al., 1990a). Mitochondrial complex I proteins within PD brains show oxidative damage and decreased electron transfer rates (Keeney et al., 2006). Patients with incidental Lewy body disease (ILBD) have levels of complex I activity that are in the middle between controls and PD patients, which are consistent with the classification of ILBD as a preclinical form of PD (Schapira et al., 1990b). The functions of other mitochondrial complexes have also been found to be decreased in sporadic PD (Bindoff et al., 1991; Haas et al., 1995; Shinde and Pasupathy, 2006; Shults et al., 1997). Mitochondrial DNA defects can also be found in PD, including mitochondrial DNA deletions in dopaminergic neurons within the substantia nigra of sporadic PD brains (Bender et al., 2006; reviewed in Martín-Jiménez et al., 2020).

Pathogenic mutations in the gene *parkin* can cause PD (AR-JP; Exner et al., 2012), but in addition, parkin dysfunction also appears to play a role in sporadic PD through its inactivation by oxidative stress (Meng et al., 2011; Wang et al., 2005), dopamine conjugation (LaVoie et al., 2005), *S*-nitrosylation (Chung et al., 2004; Yao et al., 2004), or phosphorylation (Ko et al., 2010). Parkin can be phosphorylated and inactivated by c-Abl, itself activated due to mitochondrial dysfunction and/or oxidative stress (Dawson and Dawson, 2014; Imam et al., 2011; Ko et al., 2010).

In *Drosophila melanogaster* (fruit flies), *Pink1* and *parkin* null mutant flies show phenotypes similar to PD patient symptoms, including dopaminergic neuron loss, motor defects, and some non-motor symptoms (Greene et al., 2003; Julienne et al., 2017; Park et al., 2006; Whitworth et al., 2005; Yang et al., 2006). Thus, they provide valuable model systems to investigate the mechanisms whereby mitochondrial dysfunction may be involved in PD. In this work, we explore the roles of genes encoding components of the mitochondrial respiratory complexes in PD by conducting a targeted heterozygous enhancer/suppressor screen of the *parkin* mutation in *Drosophila*.

2. Materials and methods

2.1. Drosophila strains, culture, and crosses

All *Drosophila* were reared at 25 °C on a standard cornmeal media (Formula 4–24® Instant *Drosophila* Medium, Carolina Biological Supply Company), unless otherwise stated. Controlled conditions were achieved by storing all flies and crosses in an incubator (Percival Scientific, Inc.) with a 12-h light/dark cycle. Many strains with mutations in proteins of different mitochondrial respiratory complexes were obtained from the Bloomington *Drosophila* Stock Center (BDSC stock number in parentheses): complex I: $PBac\{w^{+mC}=PB\}ND19^{c06534}$ (17768); $P\{w^{+mC} = EP\}ND42^{G4500}$ (30085); $P\{w^{+mC} = EP\}ND23^{G14097}$ (30201); complex II: $cn^1SdhA^5bw^1sp^1$ (1563); $SdhA^{1110}$ (51659); $PBac\{w^{+mC}=PB\}SdhB^{c00364}$ (10039); $P\{w^{+mC}y^{+mDint2} = EPgy2\}SdhB^{EY12081}$ (20343); complex III: $P\{w^{+mC} = EPg\}UQCR\text{-}C2^{HP30793}$ (22109); $P\{y^{+mDint2}w^{BR.E.BR} = SUPor\text{-}P\}Cyt\text{-}c1^{KG05986}ry^{506}$ (14909); complex IV: $P\{y^{+t7.7} = MaeUAS.6.11\}cype^{DP01427}$ (22073); $P\{ry^{+t7.2} = neoFRT\}82B\ COX5A^{tend}$ (33839); $PBac\{w^{+mC} = RB\}COX7A^{e03209}$ (18133); complex V: $cn^1P\{ry^{+t7.2} = PZ\}blw^1$ (11756). Other stocks obtained from the BDSC were: $park^1$ (34747); $P\{y^{+t7.7}v^{+t1.8} = TRiP.HM05104\}attP2$ (ND42 UAS-dsRNA; 28,894); $P\{y\ +\ t7.7\ v\ +\ t1.8 = TRiP.JF02700\}attP2$ (COX5A UAS-dsRNA; 27,548); $P\{w^{+mC} = GAL4\text{-}elav.L\}3$ (8760); $P\{w^{+mC} = tubP\text{-}GAL4\}LL7$ (5138). Hugo Bellen kindly supplied the stock $P\{GD6220\}V14444$ originally from Vienna *Drosophila* Resource Center (14444). The Dahomey wild type stock was kindly gifted by Barry Brogan (Newcastle University). The $park^{25}$, w^{1118}, & w^{1118} (Dahomey) flies were kindly donated by Alex Whitworth (MRC Mitochondrial Biology Unit).

For the experiments presented throughout this study, Dahomey wild type females were crossed to $park^{25}$/*TM6B* or /*TM6C* males to obtain the $park^{25}$/+ flies tested; Dahomey wild type females were similarly crossed to the mitochondrial mutant balanced males to obtain the mitochondrial mutant/+ flies tested; and the $park^{25}$/*TM6B* or /*TM6C* females were crossed to the mitochondrial mutant balanced male flies to obtain the

double heterozygote flies tested.

2.2. Climbing assays

Approximately twelve flies of each sex were anesthetized and sorted 2–3 days before a climbing assay was due to take place (to allow sufficient recovery from the effects of CO_2). Climbing assays were always performed between 9 am-1 pm and control Dahomey flies were included within each set of flies assayed in a session to account for circadian variation in locomotion (Shaw et al., 2000; Zordan et al., 2007). Flies were separated by sex due to a previously reported sex difference in climbing ability (Ali et al., 2011). Unless otherwise mentioned, flies were 2–5 days old when the climbing assays were conducted.

Flies were knocked into the climbing apparatus, which was assembled by taping two empty plastic vials together (Ali et al., 2011). Flies were given at least one minute to acclimatize before the assay began. The vial was then tapped so the flies all landed on the bottom and, due to negative geotaxis, the flies would climb. The number of flies that passed the 8 cm mark in ten seconds was recorded to assess gross motor ability. Ten trials were completed for each set of flies in each climbing assay, with at least 1 min rest between trials. The mean number of flies passing the 8 cm mark was then calculated across the ten trials and converted to a percentage of the number of flies in each vial.

Climbing assay data are presented as a normalized percent change combining independent experiments (n is number of climbing assays with the sum of all flies added together from all assays in parentheses). Repeats were done with new males and females collected from crosses. To calculate the normalized percent change, the wild type Dahomey percentages were subtracted from the percentages for each of the genotypes run in the same assay. Then that value was divided by the wild type Dahomey percentage. This resulted in the presented percent change in climbing ability vs wild type. The mean percent change, as well as the standard error of the mean (SEM), was then calculated from climbing assays conducted on different days. These means and associated SEMs were used to make the graphs for Figs. 1 and 2. Climbing assays were statistically analyzed using Generalized Linear Models with all climbing assay data from one complex analyzed together in one analysis assessing whether the genotype or the sex or the interaction between genotype and sex had significant differences and only when the overall category was significant, the pair-wise comparisons were analyzed and presented (Fig. 1-2). For climbing assays assessing ageing, assays were carried out at two or three time points in line with previous publications (Poddighe et al., 2013): 3–5 days, 15–20 days and 27–30 days. Flies were randomly selected from the same sample at each time point for the purpose of testing and thus repeated measures ANOVA analysis could be performed across the three time points (Fig. S2D). For a different ageing analysis, the flies were separated from the start (Fig. 3C-D) and analyzed by Generalized Linear Models.

2.3. L-dopa treatments

Crosses were started and maintained on instant fly food (see above) that was mixed with water containing either 1 mM L-Dopa or D-Dopa or control with nothing added to the water (concentrations from Cha et al., 2005). The progeny raised on these were assessed in climbing assays as detailed above at 2–5 days old and analyzed by Generalized Linear Models.

2.4. High-resolution respirometry

O_2 consumption was measured in homogenates from whole flies. Briefly, 10 flies were homogenized in mitochondrial isolation buffer (250 mM sucrose, 2 mM EGTA, 5 mM Tris-HCl pH 7.4) and filtered before being immediately used in an OROBOROS O2k oxygraph. Homogenates were incubated in assay buffer (120 mM KCl, 5 mM KH2PO4, 3 mM Hepes, 1 mM EGTA, 1 mM MgCl2, 0.2% bovine serum albumin, pH 7.2 at the same temperatures in which the flies were aged). State 4 respiration was measured by the addition of 5 mM pyruvate and 5 mM proline. State 3 was initiated with the addition of 1 mM ADP. CI-linked respiration (CI+CIII+CIV in figures) was inhibited by 0.5 μM rotenone and 20 mM glycerol 3-phosphate was added to stimulate CIII-linked respiration (CIII+CIV in figures). CIII-linked respiration was inhibited with the addition of 2.5 μM antimycin A. CIV respiration (CIV in figures) was initiated by the addition of 4 mM ascorbate and 2 mM TMPD. CIV respiration was inhibited with 0.5 mM KCN. Values were normalized to protein concentration as calculated by the Bradford method. The General Linear Model with repeated measures analysis was used to analyze the data. DDT (1 mM final concentration) was added to samples that were then flash frozen in liquid nitrogen and stored at −80 °C prior to use in citrate synthase activity measurements.

2.5. Citrate synthase assay

Citrate synthase activity was measured according to Magwere et al. (2006). In brief, 500 μl of the mitochondria isolation medium containing 1 mM DTT was added to the fly homogenates before samples were frozen at −80 °C. Next, the samples were defrosted and 50 μl of sample was diluted 1:5 in mitochondria isolation medium containing 1 mM PMSF. The rest of the sample was used to isolate mitochondria as described elsewhere (Sanz et al., 2010). The mitochondria were then diluted 1:4 in mitochondria isolation buffer containing 1 mM PMSF. Measurements were performed in a 96-well plate, in which 182 μl of fresh reaction buffer (100 mM Tris-HCl (pH 7.5) and 2.5 mM EDTA), 2 μl of 30 mM acetyl-CoA and 2 μl of 10 mM DTNB were added to each well. Finally, the samples (either the whole homogenate or isolated mitochondria) were added. The reaction was started by adding 10 μl of 10 mM oxaloacetate (OAA), and the linear increase in absorbance at 412 nm was followed for 3–4 min using a FluOstar Omega plate reader (BMG Labtech, Allmendgruen, Germany). Blanks were comprised of the same samples without the addition of OAA. Mitochondrial density was calculated by dividing the specific citrate synthase activity measured in whole-fly homogenates by the specific citrate synthase activity measured in isolated mitochondria. The Univariate Analysis of Variance (ANOVA) analysis was used to analyze the data.

2.6. Measurement of ROS in Drosophila brains

2′,7′-Dichlorofluorescein (H_2DCF) was used to detect total levels of reactive oxygen species (ROS) in adult fly brains dissected in phosphate-buffered saline (PBS). Following dissection, fly brains were incubated in 30 μM H_2DCF for 10 min before being washed 3 times with PBS and imaged immediately. Images were acquired using an LSM510 confocal microscope (Zeiss, Jena, Germany) equipped with a 10 × 0.3 NA objective as z stacks throughout the sample, using a 543 nm HeNe laser to excite H_2DCF. The Univariate Analysis of Variance (ANOVA) analysis was used to analyze the data.

2.7. Statistical analyses

Tests are described above along with their respective method. All statistical analysis was performed using SPSS (IBM). Statistical significance was defined at a p value <0.05.

3. Results

3.1. The interaction between mitochondrial dysfunction and Parkinson's disease gross motor defects varies depending on the individual mitochondrial mutation

As mitochondrial dysfunction is thought to be involved in Parkinson's disease pathology, we investigated how an array of mitochondrial electron transport chain mutations affected the gross motor defects of

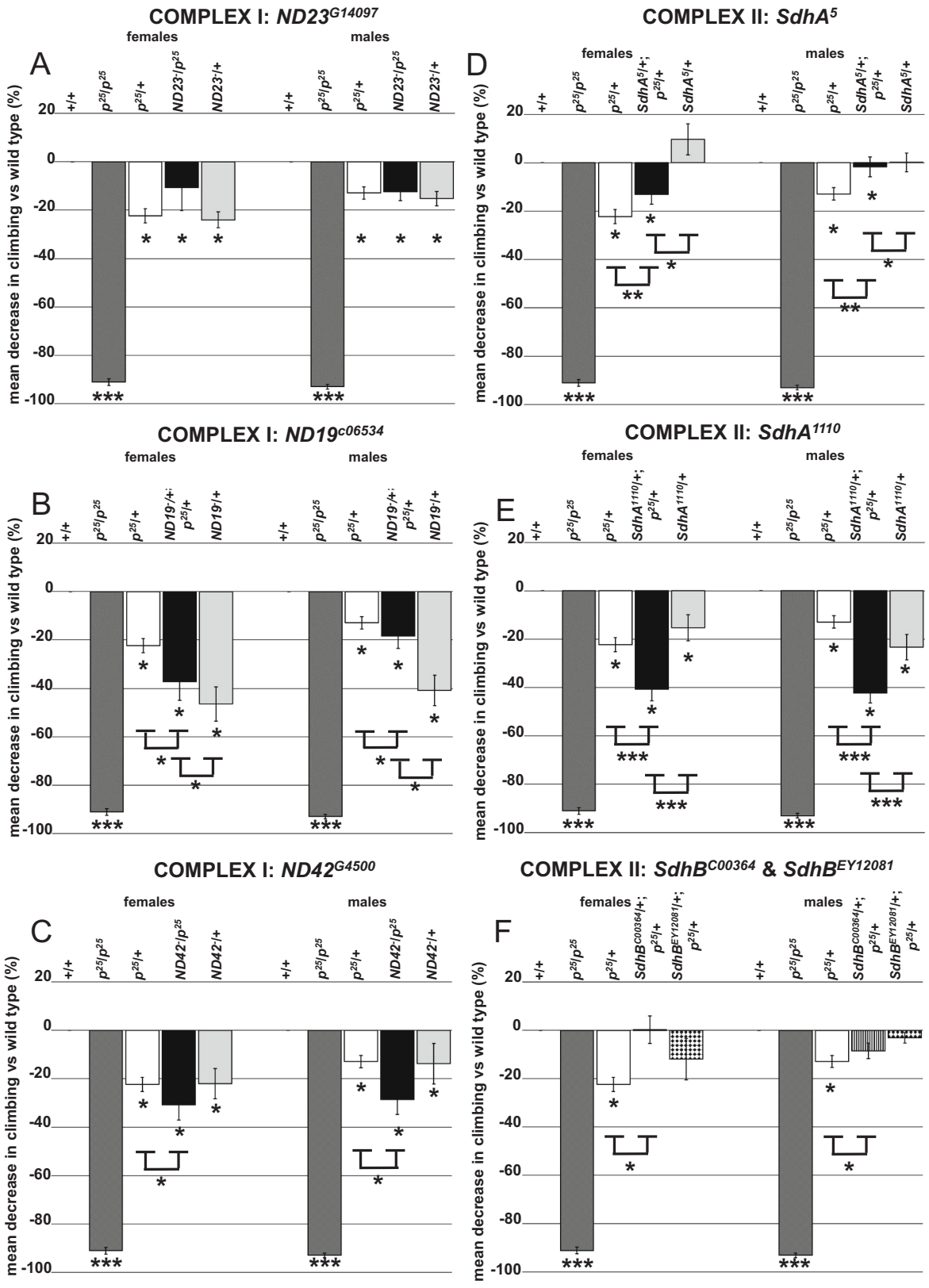

(caption on next page)

Fig. 1. Mitochondrial mutations in complex I and II have differing interactions in climbing assays with *park*^{25}. Climbing assays with *park*^{25} heterozygotes, homozygotes, and mutations in mitochondrial complex I and II ETC genes as heterozygotes or in combination with *park*^{25} with both heterozygous. Climbing assay percentages presented are normalized to the Dahomey wild type percentages within each assay (see Methods). *park*^{25}/*park*^{25} and *park*^{25}/+ data are the same in all graphs in Figs. 1 and 2, presented for direct comparison for each mitochondrial mutation: + = wild type chromosome; *p*^{25} = *park*^{25}; other mutant alleles are detailed as follows; n = number of climbing assays (number of flies), *park*^{25}/*park*^{25} females *n* = 12 (120) & males *n* = 13 (128); *park*^{25}/+ females *n* = 38 (413) & males n = 38 (422). A. Complex I: *ND23*^{G14097}: *ND23*^{G14097}/*park*^{25} females *n* = 8 (82) & males n = 8 (79); *ND23*^{G14097}/+ females n = 8 (82) & males n = 8 (79). B. Complex I: *ND19*^{c06534}: *ND19*^{c06534}/+; *park*^{25}/+ females *n* = 6 (61) & males n = 6 (58); *ND19*^{c06534}/+ females n = 6 (65) & males n = 6 (62). C. Complex I: *ND42*^{G4500}: *ND42*^{G4500}/*park*^{25} females n = 6 (61) & males n = 6 (61); *ND42*^{G4500}/+ females n = 6 (58) & males n = 6 (64). D. Complex II: *SdhA*^{5}: *SdhA*^{5}/+; *park*^{25}/+ females *n* = 11 (99) & males n = 11 (102); *SdhA*^{5}/+ females n = 11 (106) & males n = 11 (101). *E. complex* II: *SdhA*^{1110}: *SdhA*^{1110}/+; *park*^{25}/+ females *n* = 10 (85) & males n = 10 (90); *SdhA*^{1110}/+ females n = 10 (100) & males n = 10 (89). F. Complex II: *SdhB*: *SdhB*^{C00364}/+; *park*^{25}/+ females *n* = 5 (53) & males n = 5 (52); *SdhB*^{EY12081}/+; *park*^{25}/+ females *n* = 4 (38) & males n = 4 (35). Asterisks indicate a *p*-value of * <0.05, ** < 0.01, *** < 0.001 when genotype is compared to control Dahomey wild types. The asterisks mean the same when a comparison between experimental genotypes is indicated. Error bars indicate Standard Error of the Mean (SEM).

the null *parkin* mutation *park*^{25} (Greene et al., 2003; Whitworth et al., 2005) in *Drosophila melanogaster* (Fig. 1-2). The mitochondrial mutations chosen were those readily available from the Bloomington *Drosophila* Stock Center (Indiana, USA) that were homozygous lethal, as we wanted to evaluate strong mutations as heterozygotes. We found that when we crossed the mitochondrial mutations to the PD mutations, with both mutations heterozygous, no lethality was seen (data not shown).

We used the negative geotaxis (or climbing) assay (adjusted from Ali et al., 2011) as a simple measure of motor defects as it appeared to be robust, sensitive to genetic mutations, and dependent on the dopaminergic neurons that are affected in PD (Srivastav et al., 2015). The flies heterozygous for both the mitochondrial mutation and the *park*^{25} mutation were compared to the control wild type Dahomey flies, the mitochondrial heterozygotes, and the *park*^{25} heterozygotes to assess the interaction between each mitochondrial mutation and the *park*^{25} mutation (Fig. 1-2). Heterozygotes of the *park*^{25} mutation have not been often compared to wild types but are rather usually used as the control in comparison to the *park*^{25} homozygotes. This may be because commonly used control wild types climb badly, including Canton-S, Oregon-R, and *w*^{1118} (data not shown). Using a different locomotor assay, researchers have found no difference between *w*^{1118} flies and *park*^{25} heterozygotes in the *w*^{1118} background (Aggarwal et al., 2019). We found that the parental *w*^{1118} control flies climbed significantly worse than the *park*^{25} heterozygotes in the *w*^{1118} background than rather than the other way around, showing that the *w*^{1118} flies do not climb well and do not work as a control for climbing assays when using *park*^{25} heterozygotes (Fig. S1). We were aware that the Dahomey strain of controls showed better climbing ability. In climbing assays using both Dahomey and *w*^{1118} (Dahomey) – white-eyed flies in a Dahomey background, we found that *park*^{25} heterozygotes in those backgrounds climbed significantly worse when compared to the parental control (Fig. S1) and therefore used the Dahomey strain as the control wild type throughout this work.

Female and male flies that are homozygous for the *park*^{25} mutation have very little ability to climb, even at the early time point of 2–5 days after eclosion as adults (genotype overall effect: $\chi^2(2) = 1850.3$, $p < 0.001$; Dahomey vs *park*^{25}/*park*^{25}, $p < 0.001$; Fig. 1-2), consistent with previous studies (Greene et al., 2003). Heterozygous *park*^{25} flies show a significant decrease in climbing assay ability when compared to wild types (Dahomey vs *park*^{25}/+, $p < 0.001$; Fig. 1-2).

The three mitochondrial complex I mutations tested (*ND23*^{G14097}, *ND19*^{c06534}, & *ND42*^{G4500}) are significantly decreased in their climbing assay ability as heterozygotes (genotype overall effect: $\chi^2(6) = 39.7$, $p < 0.05$; Fig. 1A-C) and in combination with *park*^{25} (*ND23*^{G14097}/*park*^{25}, *ND19*^{c06534}/+; *park*^{25}/+, & *ND42*^{G4500}/*park*^{25}, $p < 0.05$; Fig. 1A-C) when compared to the Dahomey wild types, though the magnitude of the decrease varies by specific mutation. The females climbed significantly worse than the males in the overall analysis (sex overall effect: $\chi^2(1) = 9.8$, $p = 0.002$, Fig. 1A-C), however, the genotype effects were the same in males and females in the complex I analysis (sex*genotype interaction was not significant). Interestingly, the *ND23*^{G14097}/*park*^{25} double heterozygote flies did not climb significantly differently from the *park*^{25} or the *ND23*^{G14097} individual heterozygotes, lacking an enhancer or suppressor effect (Fig. 1A). In contrast, the *ND19*^{c06534}/+; *park*^{25}/+ flies climbed significantly worse than the *park*^{25} individual heterozygotes ($p < 0.05$) and significantly better than the *ND19*^{c06534} individual heterozygotes ($p < 0.05$), enhancing the *park*^{25}/+ defect and suppressing the *ND19*^{c06534}/+ defect ($p < 0.001$; Fig. 1B). Finally, the *ND42*^{G4500}/*park*^{25} double heterozygotes climbed significantly worse than the *park*^{25}/+ individual heterozygotes ($p < 0.05$), enhancing the *park*^{25}/+ defect, while not climbing significantly differently from the *ND42*^{G4500}/+ individual heterozygotes. Thus, some complex I mutations can function as enhancers of the *park*^{25}/+ climbing assay defect (Fig. 1B-C).

The two complex II genes, for which we tested 2 different mutations each, showed different interactions with *park*^{25}, which was the same in males and females (genotype overall effect: $\chi^2(6) = 106.0$, $p < 0.001$; sex overall effect and sex*genotype interaction both not significant; Fig. 1D-F). For the *SdhA* gene, the *SdhA*^{5} allele is less severe than the *SdhA*^{1110} allele, shown in the unaffected climbing of the *SdhA*^{5}/+ flies with no significant difference when compared to wild type (Fig. 1D) while the *SdhA*^{1110}/+ flies show a significant decrease in climbing ability from wild type flies ($p < 0.05$; Fig. 1E). When *SdhA*^{5} is crossed to *park*^{25}, there is a slight rescue of *park*^{25} (*SdhA*^{5}/+; *park*^{25}/+ vs *park*^{25}/+, $p < 0.01$; Fig. 1D). For *SdhA*^{1110}, there is a significant decrease compared to *park*^{25}/+ (*SdhA*^{1110}/+; *park*^{25}/+ vs *park*^{25}/+, $p < 0.001$; Fig. 1E). However, both *SdhA* individual heterozygotes show a significant decrease in climbing ability when crossed to *park*^{25} (*SdhA*^{5}/+; *park*^{25}/+ vs *SdhA*^{5}/+, $p < 0.05$; Fig. 1D; *SdhA*^{1110}/+; *park*^{25}/+ vs *SdhA*^{1110}/+, $p < 0.001$; Fig. 1E). Thus, when compared to the *SdhA*/+ single heterozygote for each, there is a decrease when crossed to *park*^{25}. For the other complex II gene assessed (*SdhB*), again there are differences based on allele, as *SdhB*^{C00364} shows a significant increase in combination with *park*^{25} (*SdhB*^{C00364}/+; *park*^{25}/+ vs *park*^{25}/+, $p < 0.05$; Fig. 1F) while *SdhB*^{EY12081} shows no significant difference (Fig. 1F). Unfortunately, it was not possible to evaluate the individual *SdhB* alleles as heterozygotes for comparison as the *CyO* balancer did not show the curly phenotype, while eye color mutations made the double heterozygotes clear, the single heterozygotes were not. In brief, individual mutations in SdhA and SdhB can function as enhancers and suppressors of the *park*^{25}/+ decrease in climbing assay ability (Fig. 1D-F).

The two complex III mutations we tested showed significant differences between genotypes (genotype overall effect: $\chi^2(4) = 58.9$, $p < 0.001$) and sexes (sex overall effect: $\chi^2(1) = 20.4$, $p < 0.001$), with the females climbing significantly worse than the males (Fig. 2A-B). There was also a significant interaction between sex and genotype ($\chi^2(1) = 20.4$, $p < 0.001$), so the males and females are considered separately (Fig. 2A-B). The *park*^{25}/+, *Cyt-c1*^{KG05986}/+, *Cyt-c1*^{KG05986}/*park*^{25} females climbed significantly worse than the Dahomey females (all $p < 0.05$; Fig. 2A). The *Cyt-c1*^{KG05986}/*park*^{25} double heterozygote females climbed significantly and strikingly worse than either the *park*^{25}/+ or the *Cyt-c1*^{KG05986}/+ individual heterozygote females, showing more than an additive effect (*Cyt-c1*^{KG05986}/*park*^{25} vs *park*^{25}/+, $p < 0.001$; *Cyt-c1*^{KG05986}/*park*^{25} vs *Cyt-c1*^{KG05986}/+, $p < 0.001$; Fig. 2A). The *park*^{25}/+ and the *Cyt-c1*^{KG05986}/*park*^{25} males climbed significantly worse than the Dahomey males (both $p < 0.05$; Fig. 2A), while the *Cyt-c1*^{KG05986}/+ males did not (Fig. 2A). The *Cyt-c1*^{KG05986}/*park*^{25} double

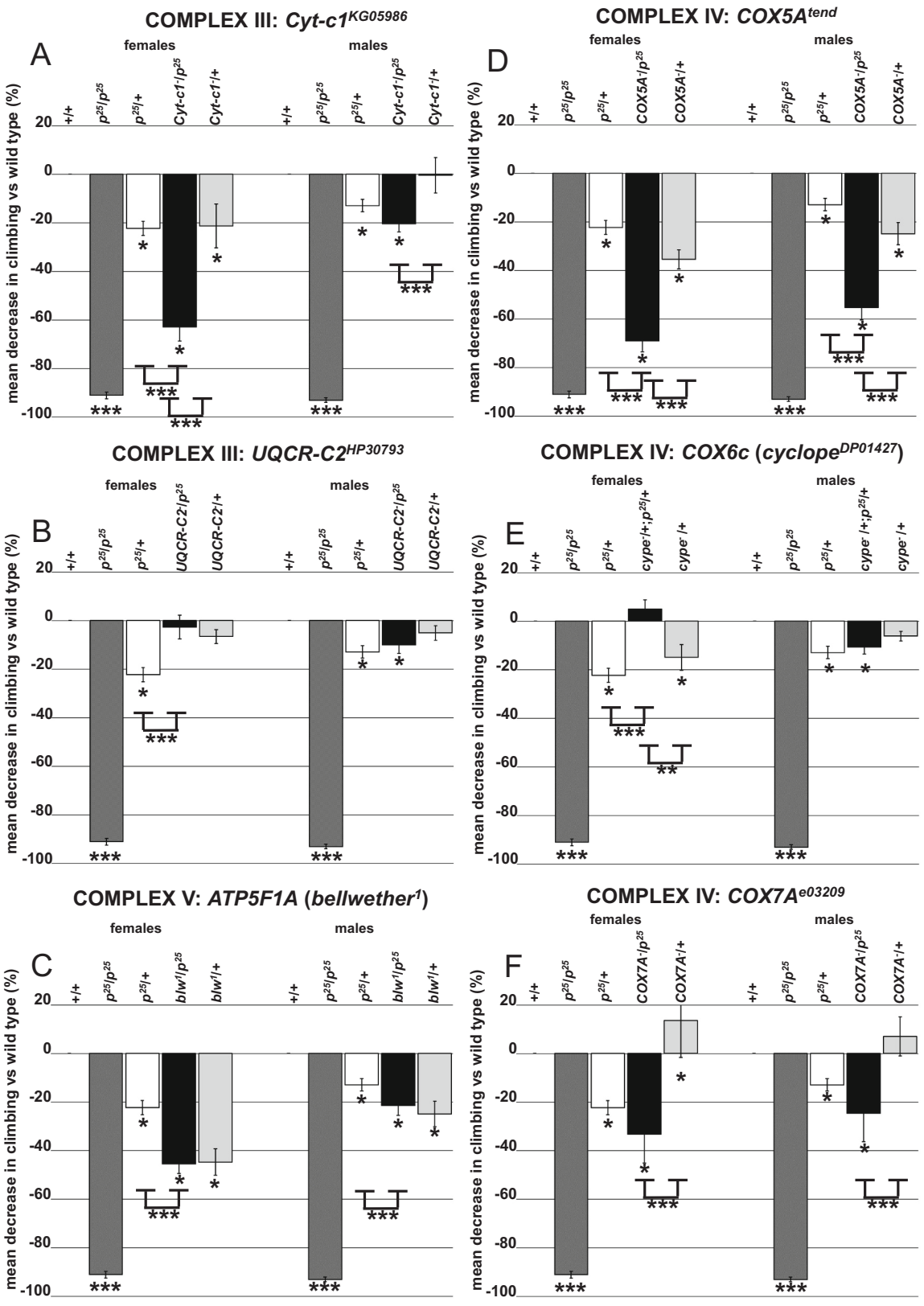

(caption on next page)

Fig. 2. Mitochondrial mutations in complex III, IV, and V have differing interactions in climbing assays with *park*^{25}. Climbing assays with *park*^{25} heterozygotes, homozygotes, and mutations in mitochondrial complex III, IV, and V genes as heterozygotes or in combination with *park*^{25} with both heterozygous. Climbing assay percentages presented are normalized to the Dahomey wild type percentages within each assay (see methods). *park*^{25}/*park*^{25} and *park*^{25}/+ data are the same in all graphs in Figs. 1 and 2, presented for direct comparison for each mitochondrial mutation: + = wild type chromosome; *p*^{25} = *park*^{25}; other mutant alleles are detailed as follows; n = number of climbing assays (number of flies), *park*^{25}/*park*^{25} females n = 12 (120) & males n = 13 (128); *park*^{25}/+ females n = 38 (413) & males n = 38 (422). A. Complex III: *Cyt-c1*^{KG05986}: *Cyt-c1*^{KG05986}/*park*^{25} females *n* = 7 (65) & males n = 6 (58); *Cyt-c1*^{KG05986}/+ females n = 8 (79) & males n = 8 (79). B. Complex III: *UQCR-C2*^{HP30793}: *UQCR-C2*^{HP30793}/*park*^{25} females *n* = 16 (160) & males n = 16 (157); *UQCR-C2*^{HP30793}/+ females n = 16 (163) & males n = 16 (163). C. Complex V: *blw*^{1}: *blw*^{1}/+; *park*^{25}/+ females n = 11 (127) & males n = 11 (121); *blw*^{1}/+ females n = 11 (130) & males n = 11 (130). D. Complex IV: *COX5A*^{tend}: *COX5A*^{tend}/*park*^{25} females n = 13 (144) & males *n* = 15 (158); *COX5A*^{tend}/+ females *n* = 21 (233) & males n = 21 (235). *E. complex* IV: *cype*^{DP01427}: *cype*^{DP01427}/+; *park*^{25}/+ females n = 12 (123) & males n = 12 (125); *cype*^{DP01427}/+ females n = 12 (133) & males n = 12 (134). F. Complex IV: *COX7A*^{e03209}: *COX7A*^{e03209}/*park*^{25} females n = 6 (55) & males n = 7 (66); *COX7A*^{e03209}/+ females n = 8 (81) & males n = 8 (83). Asterisks indicate a p-value of * <0.05, ** < 0.01, *** < 0.001 when genotype is compared to control Dahomey wild types. The asterisks mean the same when a comparison between experimental genotypes is indicated. Error bars indicate SEM.

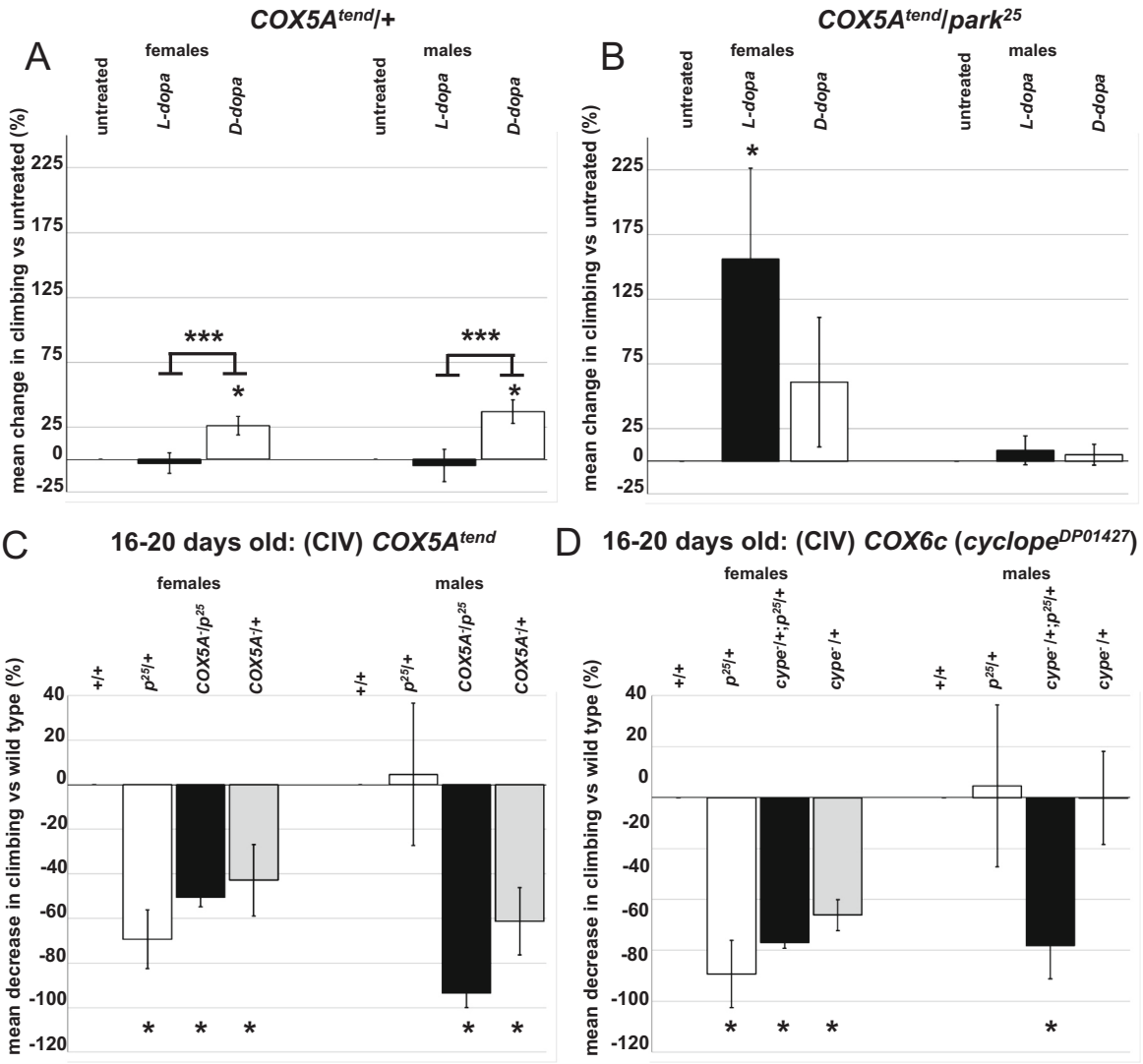

Fig. 3. Further analyses of complex IV mutations. A., B. Climbing assays with L-dopa supplementation. Climbing assay percentages presented are normalized to the untreated percentages within each assay (see methods). A. *COX5A*^{tend}/+, females n = 5 (L-dopa 56, D-dopa 58) & males n = 5 (L-dopa 55, D-dopa 58), B. *COX5A*^{tend}/*park*^{25}, females n = 4 (L-dopa 45, D-dopa 46) & males n = 5 (L-dopa 58, D-dopa 58), n = number of climbing assays (number of flies). Asterisks indicate a p-value of * <0.05, ** < 0.01, *** < 0.001 when genotype is compared to control untreated genotypes. The asterisks mean the same when a comparison between experimental genotypes is indicated. C., D. Climbing assays with 16–20-day old flies. Climbing assay percentages presented are normalized to the aged Dahomey wild type percentages within each assay (see methods). *park*^{25}/+ data are the same in C and D, presented for direct comparison for each mitochondrial mutation: + = wild type chromosome; *p*^{25} = *park*^{25}; other mutant alleles are detailed as follows; n = number of climbing assays (number of flies), *park*^{25}/+ females n = 5 (40) & males n = 4 (36). C. Complex IV: *COX5A*^{tend}: *COX5A*^{tend}/*park*^{25} females n = 2 (19) & males n = 2 (17); *COX5A*^{tend}/+ females n = 3 (34) & males n = 2 (17). D. Complex IV: *cype*^{DP01427}: *cype*^{DP01427}/+; *park*^{25}/+ females n = 3 (33) & males n = 3 (27); *cype*^{DP01427}/+ females n = 5 (59) & males n = 5 (27). Asterisks indicate a p-value of * <0.05, ** < 0.01, *** < 0.001 when genotype is compared to control Dahomey wild types. Error bars indicate SEM.

heterozygote males climbed significantly worse than the *Cyt-c1*^{KG05986}/+ individual heterozygote males (*Cyt-c1*^{KG05986}/*park*^{25} vs *Cyt-c1*^{KG05986}/+, $p < 0.05$), but not worse than the *park*^{25}/+ males, thus the effect in males is much decreased compared to the females (Fig. 2A). The *UQCR-C2*^{HP30793}/+ female and male flies do not climb significantly worse than the Dahomey males and females (Fig. 2B). In addition, the *UQCR-C2*^{HP30793}/*park*^{25} male flies climb significantly worse than the Dahomey males ($p < 0.05$), but the *UQCR-C2*^{HP30793}/*park*^{25} female flies do not climb significantly worse than Dahomey females (Fig. 2B). For the *UQCR-C2*^{HP30793}/*park*^{25} flies, the females climb significantly better than the *park*^{25}/+ females, showing a slight suppression effect ($p < 0.001$), but otherwise there are no significant differences found (Fig. 2B). In short, the interactions of complex III mutations with *park*^{25}/+ climbing assay defects are highly variable based on mutation and sex (Fig. 2A-B).

The complex IV mutations tested showed differences in climbing between genotypes (genotype overall effect: $\chi^2(6) = 210.8$, $p < 0.001$), but this effect was different for males and females (interaction effect: $\chi^2(7) = 14.9$, $p < 0.05$), so the sexes were considered separately (Fig. 2D-F). The *park*^{25}/+, *COX5A*^{tend}/*park*^{25}, and *COX5A*^{tend}/+ flies all climbed worse than the Dahomey wild type flies ($p < 0.05$). The *COX5A*^{tend}/*park*^{25} double heterozygote flies, males and females, climbed significantly and substantially worse than both of the individual heterozygote flies, in a more than simple additive manner (*COX5A*^{tend}/*park*^{25} vs *park*^{25}/+, $p < 0.001$; *COX5A*^{tend}/*park*^{25} vs *COX5A*^{tend}/+, $p < 0.001$; Fig. 2D). The *cype*^{DP01427}/+ females show a significant decrease from wild type in their climbing abilities ($p < 0.05$), though the *cype*^{DP01427}/+ males do not. The *cype*^{DP01427}/+; *park*^{25}/+ females, but not males, climb the same as wild type and significantly better than both *park*^{25}/+ females ($p < 0.001$) and *cype*^{DP01427}/+ females ($p < 0.01$), so show a considerable suppression or rescue effect of the *park*^{25}/+ climbing defects ($p < 0.001$; Fig. 2E). The *COX7A*^{e03209} heterozygote females (though not males) are actually significantly increased in climbing assay ability when compared to wild type ($p < 0.05$; Fig. 2F), while both *park*^{25}/+ and *COX7A*^{e03209}/*park*^{25} males and females are significantly decreased in climbing compared to wild type ($p < 0.05$; Fig. 2F). Thus, the *COX7A*^{e03209}/*park*^{25} clearly climb significantly worse than the *COX7A*^{e03209} heterozygotes ($p < 0.001$) but are not significantly different from the *park*^{25}/+ heterozygotes. As with the other complexes, the interaction of complex IV mutations with *park*^{25}/+ climbing ability is dependent on specific mutation assessed (Fig. 2D-F).

We also evaluated a mutation in the gene *bellwether* (*blw*^{1}) within the complex V ATP synthase, the final component of oxidative phosphorylation. It is the fly ortholog of the human gene for the ATP synthase protein ATP5A1 (Jacobs et al., 1998). In this complex V analysis, the *park*^{25}/+, *blw*^{1}/+, and *blw*^{1}/+; *park*^{25}/+ flies all climbed significantly worse than wild type (genotype overall effect: $\chi^2(2) = 28.5$, $p < 0.001$; Dahomey vs *park*^{25}/+, $p < 0.05$; Dahomey vs *blw*^{1}/+, $p < 0.05$ and Dahomey vs *blw*^{1}/+; *park*^{25}/+ $p < 0.05$; Fig. 2C). Overall, the females climbed significantly worse than the males (sex overall effect: $\chi^2(1) = 9.8$, $p = 0.002$), but the differences between genotypes were the same for males and females (no significant sex*genotype interaction; Fig. 2C). The *blw*^{1}/+ and *blw*^{1}/+; *park*^{25}/+ flies climbed significantly worse than the *park*^{25}/+ flies, but not significantly different from each other, showing that the ATP5A1 defect was worse than the *parkin* defect and was not altered by the *park*^{25}/+ mutation (*park*^{25}/+ vs *blw*^{1}/+, $p < 0.001$; *park*^{25}/+ vs *blw*^{1}/+; *park*^{25}/+, $p < 0.001$; Fig. 2C).

3.2. Decreased motor ability in females is rescued by L-dopa

Since for PD we are more interested in the effect of mitochondrial dysfunction in the brain than in muscle, we tested whether L-dopa treatment could rescue climbing assay defects (Fig. 3A-B), as this treatment has rescued *parkin* mutation climbing defects previously (Cha et al., 2005) and should be specific to dopaminergic neuron circuits, though it could have pleiotropic effects. As the *COX5A*^{tend} interaction was the strongest interaction with *park*^{25} in both males and females, this mutation was chosen to be investigated in more detail. For the *COX5A*^{tend}/+ flies, the L-dopa treatment did not significantly improve climbing ability, but the biologically inactive D-dopa treatment showed a small but significant increase in climbing compared to untreated ($p < 0.05$), as well as to the L-dopa treatment ($p < 0.001$; treatment overall effect: $\chi^2(1) = 17.69$, $p < 0.001$; Fig. 3A). There was no difference between the sexes. It is unclear why the D-dopa treatment should have an effect, however, D-dopa might interact with insect mitochondria differently than with mammalian mitochondria. For the *COX5A*^{tend}/*park*^{25} flies, there was a large and significant rescue in the climbing ability of the L-dopa treated females compared to the untreated *COX5A*^{tend}/*park*^{25} females (more than double, a 156% increase, $p < 0.05$). There was no significant difference in climbing for the L-dopa treated males or the D-dopa treated flies when compared to the untreated flies (Fig. 3B). Thus, the mitochondrial defects in *COX5A*^{tend}/+ do not appear to be rescued by L-dopa, although the PD defects caused by the *park*^{25} mutation do appear to be rescued in the *COX5A*^{tend}/*park*^{25} females (Fig. 3A-B). It is not clear why there is no improvement in the climbing ability of males, but females have generally proven to be more sensitive to alterations in genotype and treatments in this study. This suggests that the climbing assay defects we see caused by the *park*^{25} mutation are more likely caused by dopaminergic neuron dysfunction rather than muscle dysfunction, as muscle dysfunction is not likely be rescued by L-dopa treatment (Fig. 3B).

A second parkin allele was assessed and the *park*^{1} heterozygotes show a decrease in climbing assay ability similar to *park*^{25} heterozygotes (*park*^{1}/+ vs Dahomey, $p < 0.05$; Fig. S2A). The *COX5A*^{tend} flies show a decrease in climbing assay ability as heterozygotes (as previously) and in combination with *park*^{1} (Dahomey vs *COX5A*^{tend}/+, $p < 0.05$; Dahomey vs *COX5A*^{tend}/*park*^{1}, $p < 0.05$; Fig. S2A), but there is no clear interaction.

3.3. Specific knockdown of mitochondrial electron transport chain RNA decreases climbing assay ability

As a confirmation of ETC protein involvement in climbing assay dysfunction, we did a knockdown of RNA expression using hairpin RNA constructs targeted to some of the same ETC proteins evaluated above (Fig. 1C, 2D). When two different ND42 UAS-dsRNA construct lines of flies were crossed to the driver that causes ubiquitous expression of the knockdown RNA (*P{w*$^{+mC}$ *= tubP-GAL4}LL7*), the result was lethal, as would be expected when knocking out expression of an ETC protein in the whole fly (*P{y*$^{+t7.7}$*v*$^{+t1.8}$ *= TRiP.HM05104}attP2*, ND42 UAS-dsRNA, 0 of 278; *P{GD6220}v14444*, ND42 UAS-dsRNA, 0 out of 258). Besides the strong tubulin driver, there are many other GAL4 drivers in flies that can be crossed to knock down the ETC subunit RNA. The elav-GAL4 construct drives the expression of the target UAS construct only in the neurons of the flies. The elav-GAL4 > ND42 UAS-dsRNA combination caused large and significant decreases of climbing assay ability for both ND42 UAS-dsRNA lines (genotype overall effect: $F(2) = 56.4$, $p < 0.001$; Dahomey vs *ND42 UAS-dsRNA P{y*$^{+t7.7}$*v*$^{+t1.8}$ *= TRiP.HM05104}attP2/elav-GAL4*, $p < 0.001$; Dahomey vs *ND42 UAS-dsRNA P{GD6220}v14444/elav-GAL4*, $p < 0.001$; Fig. S2B). The ND42 RNA knockdowns had more of an effect on the females than the males (sex overall effect: $F(1) = 38.7$, $p < 0.001$; Fig. S2B).

As with ND42 RNA knockdowns, when the COX5A UAS-dsRNA flies are crossed to the driver that causes ubiquitous expression of the knockdown RNA (*P{w*$^{+mC}$ *= tubP-GAL4}LL7*), the result is lethal (0 flies out of 370). Again, substantial and significant decreases of climbing assay ability were seen when the elav-GAL4 neuronal driver flies were crossed with the COX5A UAS-dsRNA flies compared to the wild type Dahomey flies (genotype overall effect: $\chi^2(3) = 4181.3$, $p < 0.001$; Dahomey vs *COX5A UAS-dsRNA/elav-GAL4*, $p < 0.001$; Fig. S2C). The homozygous elav-GAL4 and *COX5A UAS-dsRNA* control flies had significant decreases in climbing assay ability compared to wild type flies (Dahomey vs *elav-GAL4/elav-GAL4*, $p < 0.001$; Dahomey vs *COX5A*

UAS-dsRNA/COX5A UAS-dsRNA, $p < 0.001$; Fig. S2C) which could be caused by the inbred background or leakage of the ds-RNA. Most importantly, the combination of the two components causes a much more severe decrease in climbing assay ability than either of the two components alone (*COX5A UAS-dsRNA/elav-GAL4* vs *elav-GAL4/elav-GAL4*, $p < 0.001$; *COX5A UAS-dsRNA/elav-GAL4* vs *COX5A UAS-dsRNA/COX5A UAS-dsRNA*, $p < 0.001$; Fig. S2C), demonstrating that a decrease in the COX5A RNA and subsequently protein, in only the neurons of the flies, has a severe effect on motor function.

Thus, targeted RNA knockdowns of two different ETC components in complex I and IV in only the neurons of the flies cause strong decreases in climbing assay ability, demonstrating that neural mitochondrial defects alone (without PD mutations) can cause motor dysfunction in fruit flies (Fig. S2B—C).

3.4. Mitochondrial dysfunction and Parkinson's defects at later time points

As Parkinson's disease gets progressively worse with age, we assessed a selection of mitochondrial mutations that already showed climbing assay deficits at 2–5 days after eclosion at later time points to see if they also got progressively worse (Fig. 3C-D, S2D). The $park^{25}/+$ females showed a significant decrease in climbing assay ability at 16–20 days old when compared to 2–5 days old ($p < 0.001$), which was more severe than the wild types, while the $park^{25}/+$ males did not show that decrease compared to wild type (genotype overall effect: $\chi^2(2) = 6.2$; Fig. 2D-E, 3C-D). The males of the $COX5A^{tend}/+$ ($p = 0.012$) and $COX5A^{tend}/park^{25}$ ($p = 0.01$) genotypes did show a significant decrease in climbing between the timepoints, the females did not (Fig. 2D, 3C). However, the lack of significant decrease in the females is likely due to a floor effect as the $COX5A^{tend}/+$ and $COX5A^{tend}/park^{25}$ are normalized to the Dahomey females (all climbing assay results are normalized to the Dahomey flies of the same sex that were run in the same assay) and the climbing ability for the Dahomey females at 16–20 days was very low to start with as the Dahomey females climbed at 40.7% at 16–20 days vs 83% at 2–5 days (actual percent that climbed) as were the $COX5A^{tend}/+$ and $COX5A^{tend}/park^{25}$ climbing percentages (Fig. 2D, 3C). Thus, a further decrease of the same magnitude is impossible. The $cype^{DP01427}/+$ females show a significant decrease in climbing at the later time point (2-5d vs 16-20d, $p = 0.002$), while the males do not (Fig. 2E, 3D). The $cype^{DP01427}/+$; $park^{25}/+$ females ($p < 0.001$) and males ($p < 0.001$) both show a significant decrease in climbing at the later time point (2-5d vs 16-20d), while the males do not (Fig. 2E, 3D). The $cype^{DP01427}$ mutation showed rescue of the climbing assay defect in females when in combination with $park^{25}$ at the 2–5-day time point but fails to rescue at the 16–20-day time point (Fig. 2E, 3D).

In a longer time-course with two of complex I subunit mutations tested at 3–5 days (Fig. 1B-C), climbing decreased significantly with age ($p < 0.001$) across all genotypes except for male $park^{25}/park^{25}$ homozygotes ($p = 0.203$, n.s.). This is likely to be a floor effect, since male $park^{25}/park^{25}$ climbing percentages were already very low at the first time point (Fig. S2D). Wild type, $park^{25}$ heterozygotes, and $ND42^{G4500}$ heterozygotes showed similar decreases in climbing assay ability as the flies got older (Fig. S2D). $ND19^{c06534}$ heterozygotes showed a significantly different decrease when compared to wild type ($p < 0.001$), though the $park^{25}/ ND42^{G4500}$ flies ($p < 0.001$) and the $park^{25}/ ND19^{c06534}$ flies ($p < 0.001$) showed stronger decreases in climbing assay ability over time (Fig. S2D). The flies that performed the worst were unsurprisingly the $park^{25}/park^{25}$ homozygotes, who did not survive long enough in adequate numbers to assess the last time point but climbed significantly worse than all the other genotypes ($p < 0.001$; Fig. S2D). Thus, we see the expected exacerbation of Parkinson's phenotypes over time, and in addition, these are affected to different degrees by mitochondrial dysfunction, depending on the particular mitochondrial mutation.

3.5. Heterozygous mitochondrial and Parkinson's mutations do not affect oxygen consumption but can decrease mitochondrial content

As in these analyses we are using flies with mitochondrial dysfunction caused by mutations in various ETC proteins, we wanted to measure the function of the ETC by assessing overall oxygen consumption. By a combination of adding complex I-, III- and IV-linked substrates and specific respiratory inhibitors, we can measure how well each complex is functioning. The flies we assessed were always heterozygous for the ETC mutations, which means they still had one normal copy of the gene, so some oxygen consumption through all the complexes was expected. The strongest enhancer found was the complex IV mutation $COX5A^{tend}$, particularly the females (Fig. 2D), thus we further analyzed these female flies for oxygen consumption. We found no significant differences in oxygen consumption compared to wild type from complexes I, III, & IV together or III & IV together or IV by itself with the $COX5A^{tend}$ heterozygotes, $park^{25}$ heterozygotes, or the heterozygous combination $COX5A^{tend}/park^{25}$ (Fig. 4A). Though the climbing assay decreases are quite strong with these females (Fig. 2D), complex IV oxygen consumption appears to be normal in all these individual and double heterozygotes. The lysates for the oxygen consumption assays are made from whole fly homogenates and most of the mitochondria measured are in muscle (Cochemé et al., 2011), while the climbing assays appear to be dependent on neurons, which could partially explain the lack of difference in oxygen consumption as could background differences.

To assess whether the lack of difference in oxygen consumption was due to variations in mitochondrial content, we estimated the activity of citrate synthase. Citrate synthase is a Kreb's cycle enzyme localized within the mitochondrial matrix and its activity is a measure of mitochondrial content. Our data shows a significant decrease in citrate synthase activity in the $COX5A^{tend}/park^{25}$ females, which implies decreased mitochondrial content, while the individual heterozygote females show no decrease (genotype overall effect: $F(3) = 3.4$, $p < 0.05$; $COX5A^{tend}/park^{25}$ vs Dahomey, $p < 0.05$; Fig. 4B). It is unclear why a decrease in overall mitochondrial content does not also result in a decrease in oxygen consumption.

3.6. Mitochondrial dysfunction increases ROS that is partially improved by parkin mutation

We are also interested in whether there are any increases in reactive oxygen species (ROS) in the brains of these flies, as this may be a possible mechanism by which mitochondrial dysfunction could cause the increased death of neurons and subsequent motor defects. By treating the dissected female brains with H_2DCF, we were able to visualize the levels of ROS in the different experimental groups (Fig. 4C-D). When the fluorescence was quantified, we saw increased levels of ROS compared to the Dahomey wild types in the $COX5A^{tend}$ heterozygotes and in the double heterozygote $COX5A^{tend}/park^{25}$ females, but not in the $park^{25}$ heterozygotes (genotype overall effect: $F(3) = 20.2$, $p < 0.001$; Dahomey vs. $COX5A^{tend}/+$, $p < 0.001$; Dahomey vs. $park^{25}/+$, n.s. $p = 1$; Dahomey vs. $COX5A^{tend}/park^{25}$, $p = 0.005$; Fig. 4C-D). It has previously been found that $park^{25}$ homozygous brains do not show an increase in ROS by H_2DCF measurement (Biosa et al., 2018) and our findings are consistent in $park^{25}$ heterozygotes, showing no increase (Fig. 4C-D). Since the $COX5A^{tend}/park^{25}$ females are the flies that have the largest decreases in climbing assay ability (Fig. 2D), we would expect them to have the highest levels of ROS, but this is not the case (Fig. 4C-D). The $COX5A^{tend}/+$ females have the highest ROS levels at almost twice the levels of wild type, while the $COX5A^{tend}/park^{25}$ females ROS levels are significantly higher than wild type but significantly lower than that of the $COX5A^{tend}/+$ females ($p = 0.001$; Fig. 4C-D). One possible explanation is based on the decrease in mitochondrial content in the $COX5A^{tend}/park^{25}$ female brains (Fig. 4B). Perhaps the ROS per mitochondrial unit could still be higher yet yield the significantly lower overall fluorescence when compared the $COX5A^{tend}$ heterozygote female brains, since the

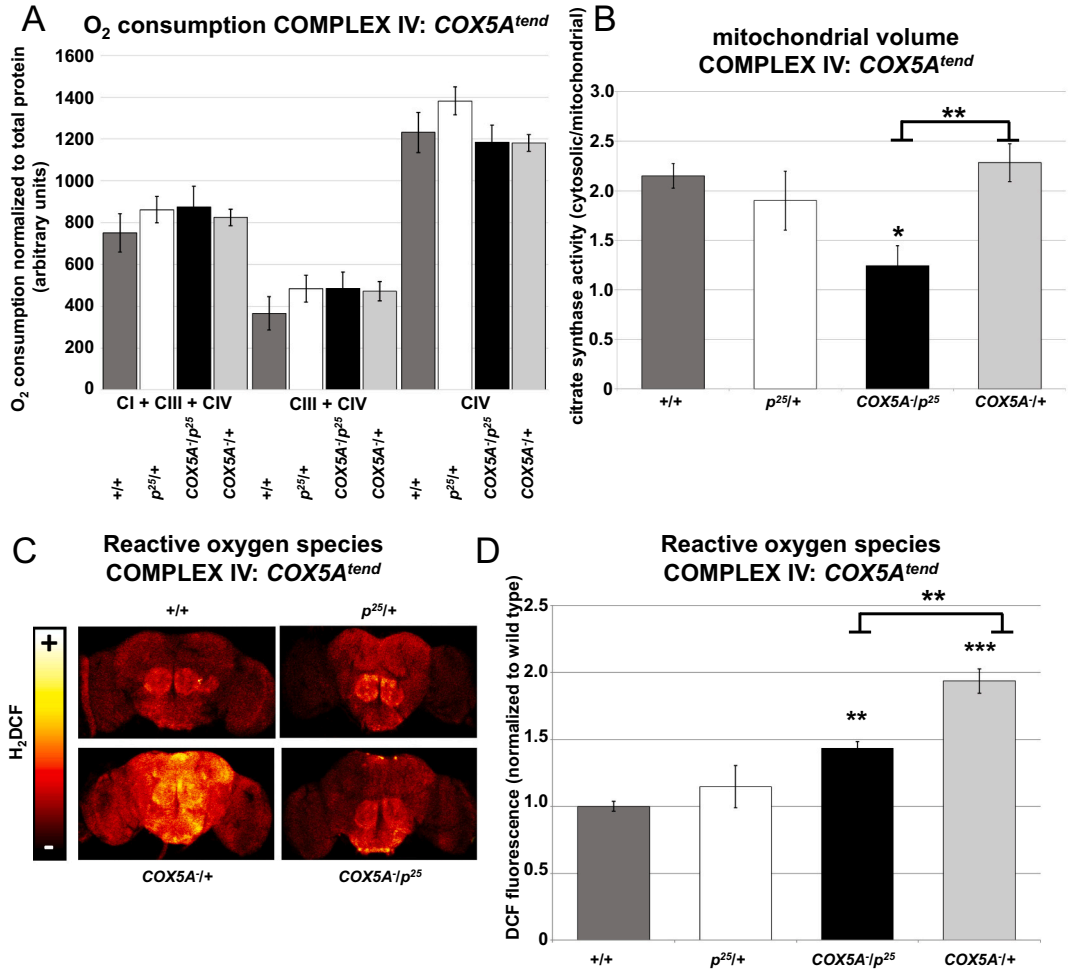

Fig. 4. Oxygen consumption, mitochondrial content, and ROS levels in *COX5A*^{tend} and *park*^{25} mutants. Only females are used in all experiments within this fig. A. Oxygen consumption normalized to protein concentration. + = wild type chromosome; p^{25} = *park*^{25}; other mutant alleles are detailed as follows. Wild type Dahomey controls n = 3, *park*^{25}/+ n = 6, *COX5A*^{tend}/+ n = 6, *COX5A*^{tend}/*park*^{25} n = 3, n = number of lysates (number of flies is 10 per lysate). B. Mitochondrial content measured by citrate synthase activity (cytosolic/mitochondrial). + = wild type chromosome; p^{25} = *park*^{25}; other mutant alleles are detailed as follows, wild type Dahomey controls n = 16, *park*^{25}/+ n = 11, *COX5A*^{tend}/+ *n* = 14, *COX5A*^{tend}/*park*^{25} n = 6, n = number of lysates (number of flies is 10 per lysate). C. Whole mount of female brains dissected and stained with H_2DCF. Lighter color is increased fluorescence. D. Quantification of H_2DCF fluorescence, including brains pictured in C., normalized to wild type. + = wild type chromosome; p^{25} = *park*^{25}; other mutant alleles are detailed as follows, wild type Dahomey controls *n* = 20, *park*^{25}/+ n = 20, *COX5A*^{tend}/+ *n* = 17, *COX5A*^{tend}/*park*^{25}*n* = 19, n = number of brains. Asterisks indicate a p-value of * <0.05, ** < 0.01, *** < 0.001 when compared to control Dahomey wild types. The asterisks mean the same when a comparison between experimental genotypes is indicated. Error bars indicate SEM.

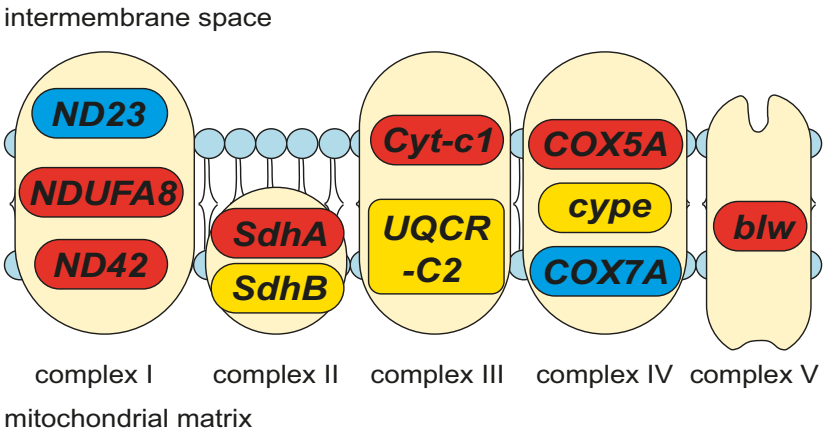

Fig. 5. Summary of mitochondrial electron transport chain mutation effects on *park*^{25} climbing ability. Schematic of inner mitochondrial membrane with the five oxidative phosphorylation complexes. Genes are indicated within a bubble describing their interaction with *park*^{25}: blue = no interaction, red = enhancer, yellow = suppressor. When there are differences between alleles or sexes, largest interaction is summarized for the gene. (For interpretation of the references to color in this figure legend, the reader is referred to the web version of this article.)

fluorescence could not be normalized to mitochondrial content within the analysis.

4. Discussion

Mitochondrial mutations, like most enzymatic defects (Kacser and Burns, 1981), are known to be subject to threshold effects (Rossignol et al., 2003; Rossignol et al., 1999). Effects on phenotype are not likely to be observed when the flies are heterozygous for a mutation (Kacser and Burns, 1981). However, combining mutations in different genes as heterozygotes should decrease function enough to overcome thresholds and identify interactions, as is seen in our results. We screened for heterozygous enhancers and suppressors of the heterozygous *park*^{25} null allele. Enhancers will likely be genes in overlapping pathways of function or additional components acting in the same pathway (Rocheleau et al., 2002). Suppressors will likely be mutations that activate alternative pathways or in negative regulators of the signalling pathways involved (Sundaram and Greenwald, 1993). A suggestion for improvement of PD neuroprotective treatments is to combine treatments from different pathways (Devos et al., 2021), so identification and characterization of different pathways involved in PD could be helpful.

Our paper identifies a number of different ETC protein subunits to be of interest in connection with PD (Fig. 5). The *park*^{25} allele is a null mutation (Greene et al., 2003) and all mitochondrial mutations were chosen as strong mutations that are lethal when homozygous. However, different mitochondrial mutation strengths could add to the variability of the effects in conjunction with the *parkin* mutation and background effects of possible other mutations on the chromosomes assessed could also add to variability. Despite these caveats, our initial screen has successfully identified strong interactions between mutations in subunits of all four ETC complexes with the *parkin* mutation, which has not been previously seen (Fig. 5). The genes we identified may be targets for modifier mutations or risk factors for PD as *parkin* mutations in patients can be heterozygous (Hattori and Mizuno, 2017).

If our identified genes are indeed PD risk factors, then they could be found in studies assessing risk factors for PD in patients. Indeed, mitochondrially-related genes are a category of genes that are found to be associated with PD (Billingsley et al., 2019). In addition, *NDUFS1*, a subunit of complex I, has been identified as being decreased in PD patients compared to control participants by both RNA-seq and proteomic analyses (Dumitriu et al., 2016). Although *NDUFS1* was not tested in this study, other complex I mutations were identified as parkin interactors in our results (Fig. 1B-C). ND19, UQCRC2, COX6C, and COX7A, identified as interactors in our study, were identified as well in the proteomic analysis as being decreased in the PD group (Dumitriu et al., 2016). The GO BP (Gene Ontology Biological Process) categories 'mitochondrial electron transport, NADH to ubiquinone' and 'respiratory electron transport chain' and the GO CC (Cellular Component) categories of 'mitochondrial respiratory chain complex I' and 'mitochondrial respiratory chain' and the GO MF (Molecular Function) category 'NADH dehydrogenase (ubiquinone) activity' were amongst the top enriched categories for proteomics related to PD (Dumitriu et al., 2016). Our findings fit into this pattern of mitochondrial influences on PD and the other mitochondrial interactors we have identified may therefore also be PD risk factors.

The mutation in the human complex I *NDUFS8* ortholog *ND23*, while decreasing climbing assay ability, did not show an interaction with the *parkin* mutation in our results (Fig. 1A), though *ND23* mutations have previously been shown to cause neurodegeneration (Cabirol-Pol et al., 2018; Loewen and Ganetzky, 2018). The mutation in the human complex I *ND19* ortholog *NDUFA8* showed a decrease in climbing assay ability and had an enhancer effect on the *parkin* mutation, oddly the combination also showed a suppression of the *ND19* decrease in our findings (Fig. 1B). Our results also show the mutation in the complex I *NDUFA10* ortholog *ND42* decreased climbing assay ability and enhanced the *parkin* climbing defect (Fig. 1C). In *Pink1* (thought to be associated with *parkin* in mitophagy and PD) fly mutants, there is a complex I deficiency which is rescued by *ND42* expression (Morais et al., 2014; Pogson et al., 2014). However, *parkin* defects were not rescued by *ND42* expression (Pogson et al., 2014), indicating a slightly different pathway of function. The ND23 subunit is found in the core or central part of complex I and is directly involved in transferring of electrons, while the ND19 and ND42 subunits are accessory subunits (Rhooms et al., 2020), which could explain the differences seen in our findings in *parkin* interaction, with the accessory subunits enhancing *parkin* defects, while the core subunit does not (Fig. 1A-C).

The two mutations we assessed in the complex II gene *SdhA* both showed an interaction with *parkin* (Fig. 1 D-E). *SdhA*^{5} and *SdhA*^{1110} are two different single amino acid change mutations that have previously shown no differences in severity, and both are homozygous lethal (Mast et al., 2008). The *SdhA*^{1110} mutation is in the N-terminal FAD-binding 2 domain, while *SdhA*^{5} mutation is in the C-terminal succinate dehydrogenase flavoprotein domain (Mast et al., 2008). We show the *SdhA*^{5} mutation when heterozygous has no decrease in climbing assay ability and reveals a slight suppression in combination with *parkin* (Fig. 1D). However, in our findings, the *SdhA*^{1110} mutation shows a decrease in climbing assay ability when heterozygous and an enhancement in combination with *parkin* (Fig. 1E). This difference in effects may be caused by the different locations of the mutations in the gene (Mast et al., 2008). However, both are consistent with the *parkin* mutation making the mitochondrial effect worse, meaning the interaction is consistent between both *SdhA* mutations and *parkin* (Fig. 1 D-E). We also found the *SdhB*^{C00364} mutation shows a slight suppressive effect with *parkin*, while the *SdhB*^{EY12081} mutation (Walker et al., 2006) does not, though since the *SdhB*^{C00364} mutation has not been characterized, it is difficult to understand the difference (Fig. 1F). Both SdhA and SdhB are catalytic core subunits of complex II and are involved in the redox reactions to transfer the electrons to ubiquinone (Rutter et al., 2010).

In the current study, the mutation in the human complex III *cytochrome c1* ortholog *Cyt-c1* decreased climbing assay ability in females, though not in males, and showed a strong interaction in females with *parkin*, though again, not in males (Fig. 2A). In our findings, the mutation in the human complex III *UQCRC2* (*ubiquinol-cytochrome c reductase core protein 2*) ortholog *UQCR-C2* also showed a *parkin* interaction in females and not in males, though the *UQCR-C2* female heterozygotes showed no climbing assay decrease and a slight suppression of parkin, while the males showed a climbing assay decrease (Fig. 2B). Both subunits Cyt-c1 and UQCR-C2 are core subunits of complex III.

The mutation in the complex IV COX5A subunit showed a decrease in climbing assay ability as heterozygotes and an even more substantial decrease in combination with *parkin* in our research (Fig. 2D). The *COX5A*^{tend} mutation has not been previously shown to interact with Parkinson's phenotypes (Mandal et al., 2005). The mutation in the human complex IV COX6c ortholog *cyclope*^{DP01427} showed a decrease in climbing assay as heterozygote females, but actually showed a suppression effect in females when crossed to the *parkin* mutation in this current study (Fig. 2E). This rescue effect has not previously been found with *cyclope* and *parkin*, though *cyclope* has been previously characterized as lethal and inhibiting cell growth (Szuplewski and Terracol, 2001). In our results, the mutation in the complex IV COX7A subunit showed an increase in climbing assay ability when heterozygous, but an enhancement of the *parkin* effect (Fig. 2F). Interestingly, targeted knockdown of COX7A in only dopaminergic neurons in flies does not have effect on motor function (Yalgin et al., 2020), so the interaction demonstrated in our work is not a simple identification of direct causal PD factors, but in combination with *parkin*. All the complex IV mutations we tested show interactions with *parkin*, rescue or enhancement (Fig. 2 D—F), and they are all thought to be regulatory subunits of complex IV, not part of the catalytic core (Kadenbach and Hüttemann, 2015).

Interestingly, there was no interaction seen with the single ortholog to the mitochondrial complex V ATP synthase (ATP5F1A) subunit, *bellwether*^{1} (Jacobs et al., 1998), we tested (Fig. 2C). There was loss of

climbing ability we saw in the mitochondrial heterozygotes that was not changed when crossed to the *parkin* mutation (Fig. 2C), indicating that loss of some ATP synthase function effects the climbing ability in such a way that precludes any *parkin* mutant defect effects. It would be interesting to see if other complex V mutations would have similar effects, though other subunits in complex V appear to have a regulatory role in mitochondrial DNA maintenance (Fukuoh et al., 2014).

Previous literature, due to data on mitochondrial complex inhibitors in PD and more, mostly implicates complex I in connection with Parkinson's disease (Borsche et al., 2021). The interaction of complex mutations other than those in complex I with *parkin* and the degree of differences between mutations in complex subunits that we observed, indicates that further research on different mitochondrial complexes and PD is necessary, with candidates highlighted in our findings (Fig. 5).

In addition, our study finds an intriguing interaction where a mutation in a complex IV gene actually rescues climbing assay ability at early time points, but not at late time points (Fig. 2E, 3D). This offers a possible target for drug discovery that might delay or otherwise ameliorate Parkinson's disease symptoms if treatment is started early. However, further investigations to characterize this rescue in pre-clinical models is necessary before any translational work can begin. A number of neuroprotective treatments have been proposed due to promising data in pre-clinical models that have not proved efficacious in patient clinical trials, but there are some steps that can be taken to improve these rates (Devos et al., 2021).

The *COX5A*^{tend} (complex IV subunit) and *parkin* double heterozygote females with the largest climbing assay decreases (Fig. 2D) do not show a decrease in oxygen consumption in our findings (Fig. 4A), suggesting that ATP production may be at normal levels. This is likely because the flies are heterozygous for both mutations, allowing for enough protein to conduct normal oxidative phosphorylation (OXPHOS). The cause of climbing assay defects in these experiments is then unlikely to be a lack of ATP. The oxygen consumption experiments were conducted on whole flies, so there could be decreases within the brain or subsets of neurons that are masked by the rest of the body. The way we measured oxygen consumption, most of the mitochondria in whole fly lysates come from the muscle (Cochemé et al., 2011). If oxidative phosphorylation could be measured in just the brains, that might show differences. Neurons use ATP at elevated levels and perhaps they are more sensitive to slight changes that would not be picked up in these assays. However, our present study found no evidence that oxygen consumption was affected (Fig. 4A).

Mitochondrial content appears to be decreased in the flies with the largest climbing assay decreases (Fig. 4B), although oxygen consumption seems to be maintained at normal levels in our current findings (Fig. 4A). This is somewhat consistent with the ROS increase seen in our study, though not completely (Fig. 4C-D). Our results show mitochondrial content is decreased in only the double heterozygote (Fig. 4B) and there is an increase in ROS in the double heterozygote (Fig. 4C-D). However, the highest increase in ROS is in the single mitochondrial heterozygote and the double heterozygote, though showing a significant increase in ROS over the wild type, shows a significant decrease compared to the single mitochondrial heterozygote in our current findings (Fig. 4C-D). Since the double heterozygote shows less mitochondrial content, perhaps that is the reason for the decreased ROS in comparison to the single mitochondrial heterozygote in our results. Another explanation for the modest increase in ROS in the double heterozygote is that the ETC is too damaged, and the ROS cannot be produced. Thus, the mechanism is complicated, but we implicate increasing levels of ROS in increased climbing defects in these PD model flies (Fig. 4C-D).

5. Conclusions

Our research has shown that mitochondrial complex I may not be the only part of the ETC that could be involved in PD and has provided some potential targets for drug discovery. Some of the subunits identified in our findings should be further investigated and, more generally, the roles of specific mitochondrial ETC subunits in PD could be important.

Availability of data and materials

The datasets used and/or analyzed during the current study are available from the corresponding author on reasonable request.

Funding

Our study was supported by Northumbria University and Teesside University. Work in AS's laboratory was funded by the European Research Council (260632-ComplexI&Ageing). The funders had no role in study design, data collection and analysis, decision to publish, or preparation of the manuscript.

CRediT authorship contribution statement

Maria E. O'Hanlon: Validation, Formal analysis, Investigation, Writing – review & editing, Visualization. **Clare Tweedy:** Methodology, Formal analysis, Investigation, Visualization. **Filippo Scialo:** Methodology, Formal analysis, Investigation, Writing – review & editing, Visualization. **Rosemary Bass:** Conceptualization, Methodology, Investigation, Resources, Writing – review & editing. **Alberto Sanz:** Conceptualization, Methodology, Resources, Writing – review & editing, Supervision, Funding acquisition. **Tora K. Smulders-Srinivasan:** Conceptualization, Methodology, Formal analysis, Investigation, Resources, Writing – original draft, Writing – review & editing, Visualization, Supervision, Project administration, Funding acquisition.

Declaration of Competing Interest

The authors declare that they have no competing interests.

Acknowledgements

We would like to acknowledge the time and effort spent by Dr. Ashwin Sriram to help TS perform experiments in the laboratory of AS.

Appendix A. Supplementary data

Supplementary data to this article can be found online at https://doi.org/10.1016/j.nbd.2022.105803.

References

Aggarwal, A., et al., 2019. A locomotor assay reveals deficits in heterozygous Parkinson's disease model and proprioceptive mutants in adult Drosophila. Proc. Natl. Acad. Sci. U. S. A. 116, 24830–24839.
Ali, Y.O., et al., 2011. Assaying Locomotor, Learning, and Memory Deficits in Drosophila Models of Neurodegeneration, p. e2504.
Bender, A., et al., 2006. High levels of mitochondrial DNA deletions in substantia nigra neurons in aging and Parkinson disease. Nat. Genet. 38, 515–517.
Billingsley, K.J., et al., 2019. Mitochondria function associated genes contribute to Parkinson's disease risk and later age at onset. Npj Parkinson's Disease. 5, 8.
Bindoff, L.A., et al., 1991. Respiratory chain abnormalities in skeletal muscle from patients with Parkinson's disease. J. Neurol. Sci. 104, 203–208.
Biosa, A., et al., 2018. Superoxide dismutating molecules rescue the toxic effects of PINK1 and parkin loss. Hum. Mol. Genet. 27, 1618–1629.
Borsche, M., et al., 2021. Mitochondria and Parkinson's disease: clinical, molecular, and translational aspects. J. Parkinsons Dis. 11, 45–60.
Bose, A., Beal, M.F., 2016. Mitochondrial dysfunction in Parkinson's disease. J. Neurochem. 139 (Suppl 1), 216–231.
Cabirol-Pol, M.-J., et al., 2018. Glial lipid droplets and neurodegeneration in a Drosophila model of complex I deficiency. Glia. 66, 874–888.
Caparros-Lefebvre, D., Elbaz, A., 1999. Possible relation of atypical parkinsonism in the French West Indies with consumption of tropical plants: a case-control study. Lancet 354, 281–286.
Cha, G.-H., et al., 2005. Parkin negatively regulates JNK pathway in the dopaminergic neurons of Drosophila. Proc. Natl. Acad. Sci. U. S. A. 102, 10345–10350.

Champy, P., et al., 2004. Annonacin, a lipophilic inhibitor of mitochondrial complex I, induces nigral and striatal neurodegeneration in rats: possible relevance for atypical parkinsonism in Guadeloupe. J. Neurochem. 88, 63–69.
Chung, K.K.K., et al., 2004. S-Nitrosylation of Parkin regulates ubiquitination and compromises Parkin's protective function. Science. 304, 1328–1331.
Cochemé, Helena M., et al., 2011. Measurement of H₂O₂ within living Drosophila during aging using a Ratiometric mass spectrometry probe targeted to the mitochondrial matrix. Cell Metab. 13, 340–350.
Dauer, W., et al., 2002. Resistance of α-synuclein null mice to the parkinsonian neurotoxin MPTP. Proc. Natl. Acad. Sci. 99, 14524–14529.
Davis, G.C., et al., 1979. Chronic parkinsonism secondary to intravenous injection of meperidine analogues. Psychiatry Res. 1, 249–254.
Dawson, T.M., Dawson, V.L., 2014. Parkin plays a role in sporadic Parkinson's disease. Neurodegener. Dis. 13, 69–71.
Devos, D., et al., 2021. Seven solutions for neuroprotection in Parkinson's disease. Mov. Disord. 36, 306–316.
Dumitriu, A., et al., 2016. Integrative analyses of proteomics and RNA transcriptomics implicate mitochondrial processes, protein folding pathways and GWAS loci in Parkinson disease. BMC Med. Genet. 9, 5.
Exner, N., et al., 2012. Mitochondrial dysfunction in Parkinson's disease: molecular mechanisms and pathophysiological consequences. EMBO J. 31, 3038–3062.
Fukuoh, A., et al., 2014. Screen for mitochondrial DNA copy number maintenance genes reveals essential role for ATP synthase. Mol. Syst. Biol. 10, 734.
Greene, J.C., et al., 2003. Mitochondrial pathology and apoptotic muscle degeneration in Drosophila parkin mutants. Proc. Natl. Acad. Sci. U. S. A. 100, 4078–4083.
Haas, R.H., et al., 1995. Low platelet mitochondrial complex I and complex II/III activity in early untreated parkinson's disease. Ann. Neurol. 37, 714–722.
Hall, A., et al., 2020. Genetic risk profiling in Parkinson's disease and utilizing genetics to gain insight into disease-related biological pathways. Int. J. Mol. Sci. 21.
Hattori, N., Mizuno, Y., 2017. Twenty years since the discovery of the parkin gene. J. Neural 124 (9), 1037–1054 (Transmission).
Imai, Y., 2020. PINK1-Parkin signaling in Parkinson's disease: lessons from Drosophila. Neurosci. Res. 159, 40–46.
Imam, S.Z., et al., 2011. Novel regulation of Parkin function through c-Abl-mediated tyrosine phosphorylation: implications for Parkinson's disease. J. Neurosci. 31, 157–163.
Jacobs, H., et al., 1998. A screen for lethal mutations in the chromosomal region 59AB suggests that bellwether encodes the alpha subunit of the mitochondrial ATP synthase in Drosophila melanogaster. Mol. Gen. Genet. MGG 259, 383–387.
Julienne, H., et al., 2017. Drosophila PINK1 and parkin loss-of-function mutants display a range of non-motor Parkinson's disease phenotypes. Neurobiol. Dis. 104, 15–23.
Kacser, H., Burns, J.A., 1981. The molecular basis of dominance. Genetics. 97, 639–666.
Kadenbach, B., Hüttemann, M., 2015. The subunit composition and function of mammalian cytochrome c oxidase. Mitochondrion. 24, 64–76.
Keane, P.C., et al., 2011. Mitochondrial Dysfunction in Parkinson's Disease. Parkinson's Disease 2011.
Keeney, P.M., et al., 2006. Parkinson's disease brain mitochondrial complex I has Oxidatively damaged subunits and is functionally impaired and misassembled. J. Neurosci. 26, 5256–5264.
Kitada, T., et al., 1998. Mutations in the parkin gene cause autosomal recessive juvenile parkinsonism. Nature. 392, 605–608.
Klivenyi, P., et al., 2006. Mice lacking alpha-synuclein are resistant to mitochondrial toxins. Neurobiol. Dis. 21, 541–548.
Ko, H.S., et al., 2010. Phosphorylation by the c-Abl protein tyrosine kinase inhibits parkin's ubiquitination and protective function. Proc. Natl. Acad. Sci. 107, 16691–16696.
Langston, J.W., et al., 1983. Chronic parkinsonism in humans due to a product of meperidine-analog synthesis. Science. 219, 979–980.
Langston, J.W., et al., 1999. Evidence of active nerve cell degeneration in the substantia nigra of humans years after 1-methyl-4-phenyl-1,2,3,6-tetrahydropyridine exposure. Ann. Neurol. 46, 598–605.
Lannuzel, A., et al., 2003. The mitochondrial complex i inhibitor annonacin is toxic to mesencephalic dopaminergic neurons by impairment of energy metabolism. Neuroscience. 121, 287–296.
LaVoie, M.J., et al., 2005. Dopamine covalently modifies and functionally inactivates parkin. Nat. Med. 11, 1214–1221.
Loewen, C.A., Ganetzky, B., 2018. Mito-nuclear interactions affecting lifespan and neurodegeneration in a Drosophila model of Leigh syndrome. Genetics. 208, 1535–1552.
Magwere, T., et al., 2006. The effect of dietary restriction on mitochondrial protein density and flight muscle mitochondrial morphology in Drosophila. J. Gerontol. Ser. A Biol. Med. Sci. 61, 36–47.
Mandal, S., et al., 2005. Mitochondrial regulation of cell cycle progression during development as revealed by the tenured mutation in Drosophila. Dev. Cell 9, 843–854.
Martín-Jiménez, R., et al., 2020. Damage in mitochondrial DNA associated with Parkinson's disease. DNA Cell Biol. 39, 1421–1430.
Mast, J.D., et al., 2008. Reactive oxygen species act remotely to cause synapse loss in a Drosophila model of developmental mitochondrial encephalopathy. Development. 135, 2669–2679.
Meng, F., et al., 2011. Oxidation of the cysteine-rich regions of parkin perturbs its E3 ligase activity and contributes to protein aggregation. Mol. Neurodegener. 6, 34.
Morais, V.A., et al., 2014. PINK1 loss-of-function mutations affect mitochondrial complex I activity via NdufA10 ubiquinone uncoupling. Science. 344, 203–207.
Nieto, M., et al., 2006. Increased sensitivity to MPTP in human α-synuclein A30P transgenic mice. Neurobiol. Aging 27, 848–856.
Park, J., et al., 2006. Mitochondrial dysfunction in Drosophila PINK1 mutants is complemented by parkin. Nature. 441, 1157–1161.
Parker Jr., W.D., et al., 2008. Complex I deficiency in Parkinson's disease frontal cortex. Brain Res. 1189, 215–218.
Poddighe, S., et al., 2013. Impaired sense of smell in a Drosophila Parkinson's model. PLoS One 8, e73156.
Pogson, J.H., et al., 2014. The complex I subunit NDUFA10 selectively rescues Drosophila pink1 mutants through a mechanism independent of mitophagy. PLoS Genet. 10, e1004815.
Polymeropoulos, M.H., et al., 1997. Mutation in the α-Synuclein gene identified in families with Parkinson's disease. Science. 276, 2045–2047.
Ramsay, R.R., et al., 1986. Inhibition of mitochondrial NADH dehydrogenase by pyridine derivatives and its possible relation to experimental and idiopathic parkinsonism. Biochem. Biophys. Res. Commun. 135, 269–275.
Rhooms, S.-K., et al., 2020. Insights from Drosophila on mitochondrial complex I. Cell. Mol. Life Sci. 77, 607–618.
Rocha, E.M., et al., 2018. Alpha-synuclein: pathology, mitochondrial dysfunction and neuroinflammation in Parkinson's disease. Neurobiol. Dis. 109, 249–257.
Rocheleau, C.E., et al., 2002. A lin-45 raf enhancer screen identifies eor-1, eor-2 and unusual alleles of Ras pathway genes in Caenorhabditis elegans. Genetics. 161, 121–131.
Rodríguez-Nogales, C., et al., 2016. Brain aging and Parkinson's disease: new therapeutic approaches using drug delivery systems. Maturitas. 84, 25–31.
Rossignol, R., et al., 1999. Threshold effect and tissue specificity: IMPLICATION FOR MITOCHONDRIAL CYTOPATHIES. J. Biol. Chem. 274, 33426–33432.
Rossignol, R., et al., 2003. Mitochondrial threshold effects. Biochem. J. 370, 751–762.
Rutter, J., et al., 2010. Succinate dehydrogenase – assembly, regulation and role in human disease. Mitochondrion. 10, 393–401.
Sanz, A., et al., 2010. Expression of the yeast NADH dehydrogenase Ndi1 in Drosophila confers increased lifespan independently of dietary restriction. Proc. Natl. Acad. Sci. U. S. A. 107, 9105–9110.
Schapira, A.H., 2010. Complex I: inhibitors, inhibition and neurodegeneration. Exp. Neurol. 224, 331–335.
Schapira, A.H.V., et al., 1990a. Mitochondrial complex I deficiency in Parkinson's disease. J. Neurochem. 54, 823–827.
Schapira, A.H.V., et al., 1990b. Anatomic and disease specificity of NADH CoQ1 reductase (complex I) deficiency in Parkinson's disease. J. Neurochem. 55, 2142–2145.
Shaw, P.J., et al., 2000. Correlates of sleep and waking in Drosophila melanogaster. Science. 287, 1834–1837.
Shimura, H., et al., 2000. Familial Parkinson disease gene product, parkin, is a ubiquitin-protein ligase. Nat. Genet. 25, 302–305.
Shinde, S., Pasupathy, K., 2006. Respiratory-chain enzyme activities in isolated mitochondria of lymphocytes from patients with Parkinson's disease: preliminary study. Neurol. India 54, 390–393.
Shults, C.W., et al., 1997. Coenzyme Q10 levels correlate with the activities of complexes I and II/III in mitochondria from parkinsonian and nonparkinsonian subjects. Ann. Neurol. 42, 261–264.
Song, D.D., et al., 2004. Enhanced substantia nigra mitochondrial pathology in human α-synuclein transgenic mice after treatment with MPTP1. Exp. Neurol. 186, 158–172.
Spillantini, M.G., et al., 1997. [alpha]-Synuclein in Lewy bodies. Nature. 388, 839–840.
Srivastav, S., et al., 2015. Folic acid supplementation rescues anomalies associated with knockdown of parkin in dopaminergic and serotonergic neurons in Drosophila model of Parkinson's disease. Biochem. Biophys. Res. Commun. 460, 780–785.
Sundaram, M., Greenwald, I., 1993. Suppressors of a lin-12 hypomorph define genes that interact with both lin-12 and glp-1 in Caenorhabditis elegans. Genetics. 135, 765–783.
Szuplewski, S., Terracol, R., 2001. The cyclope gene of Drosophila encodes a cytochrome c oxidase subunit VIc homolog. Genetics. 158, 1629–1643.
Valente, E.M., et al., 2004. Hereditary early-onset Parkinson's disease caused by mutations in PINK1. Science. 304, 1158–1160.
Van Den Eeden, S.K., et al., 2003. Incidence of Parkinson's disease: variation by age, gender, and race/ethnicity. Am. J. Epidemiol. 157, 1015–1022.
Vos, M., et al., 2021. Ceramide accumulation induces mitophagy and impairs β-oxidation in PINK1 deficiency. Proc. Natl. Acad. Sci. 118, e2025347118.
Walker, D.W., et al., 2006. Hypersensitivity to oxygen and shortened lifespan in a Drosophila mitochondrial complex II mutant. Proc. Natl. Acad. Sci. 103, 16382–16387.
Wang, C., et al., 2005. Stress-induced alterations in parkin solubility promote parkin aggregation and compromise parkin's protective function. Hum. Mol. Genet. 14, 3885–3897.
Wang, X., et al., 2019. Pathogenic alpha-synuclein aggregates preferentially bind to mitochondria and affect cellular respiration. Acta Neuropathol Commun. 7, 41.
Whitworth, A.J., et al., 2005. Increased glutathione S-transferase activity rescues dopaminergic neuron loss in a Drosophila model of Parkinson's disease. Proc. Natl. Acad. Sci. 102, 8024–8029.
Yalgin, C., et al., 2020. Effects on dopaminergic neurons are secondary in COX-deficient locomotor dysfunction in Drosophila. iScience 23.

Yang, Y., et al., 2006. Mitochondrial pathology and muscle and dopaminergic neuron degeneration caused by inactivation of Drosophila Pink1 is rescued by Parkin. Proc. Natl. Acad. Sci. 103, 10793–10798.
Yao, D., et al., 2004. Nitrosative stress linked to sporadic Parkinson's disease: S-nitrosylation of parkin regulates its E3 ubiquitin ligase activity. Proc. Natl. Acad. Sci. U. S. A. 101, 10810–10814.
Zordan, M.A., et al., 2007. Monitoring and analyzing Drosophila circadian locomotor activity. In: Rosato, E. (Ed.), Circadian Rhythms: Methods and Protocols. Humana Press, Totowa, NJ, pp. 67–81.